JOURNAL OF GEOPHYSICAL RESEARCH, VOL. 108, NO. D10, 4307, doi:10.1029/2002JD002903, 2003

# Two-day wave observations of UARS Microwave Limb Sounder mesospheric water vapor and temperature

Varavut Limpasuvan
Department of Chemistry and Physics, Coastal Carolina University, Conway, South Carolina, USA

Dong L. Wu
Jet Propulsion Laboratory, California Institute of Technology, Pasadena, California, USA

Received 1 September 2002; revised 21 January 2003; accepted 4 March 2003; published 22 May 2003.

[1] A two-day wave disturbance is observed in the mesospheric temperature and water vapor on the basis of new version data from the Upper Atmosphere Research Satellite Microwave Limb Sounder. Using two data segments during the austral summers (January–February of 1992 and 1993) and the asynoptic mapping method, a strong wave signal is identified as having zonal wave number 3 and a westward period of about 2.1 days. The wave amplitudes are located near the core of the summer easterly jet with strongest wave amplitudes (as large as 11 K and 0.35 part per million by volume) near the mesopause. The temperature and water vapor wave strengths are highly correlated in time, but their peaks are almost longitudinally out of phase. Poleward heat flux associated with upward wave energy propagation in the Southern Hemisphere points to baroclinic instability as the cause for the wave appearance. A growing wave signature in water vapor is observed in regions of strong meridional gradient of water vapor. Near the mesopause, wave breaking is suggested as moist polar air is displaced into the much drier subtropics and wave amplitude decays. *INDEX TERMS:* 3332 Meteorology and Atmospheric Dynamics: Mesospheric dynamics; 3334 Meteorology and Atmospheric Dynamics: Middle atmosphere dynamics (0341, 0342); 3384 Meteorology and Atmospheric Dynamics: Waves and tides; *KEYWORDS:* middle atmosphere dynamics, mesosphere water vapor, mesosphere temperature, two-day wave, mesospheric waves

**Citation:** Limpasuvan, V., and D. L. Wu, Two-day wave observations of UARS Microwave Limb Sounder mesospheric water vapor and temperature, *J. Geophys. Res.*, 108(D10), 4307, doi:10.1029/2002JD002903, 2003.

## 1. Introduction

[2] The two-day wave is a recurring phenomenon, readily observed just after the solstice. The wave can be found in the upper stratosphere up through the thermosphere and typically persists for 15–30 days. As a zonal wave number 3 disturbance that propagates westward with a period of about 2 days, the wave amplitude resides in close proximity to the summer easterly jet core where the vertical and meridional wind shears are very strong. As such, its existence has been attributed to the instability of the summer easterly jet [e.g., *Plumb*, 1983; *Pfister*, 1985; *Randel*, 1994]. Because of its recurring nature and lack of known forcing mechanisms, the two-day wave has also been suggested to be a zonal wave number 3 Rossy-gravity global normal mode with large amplification in the summer hemisphere under the solstice condition [*Salby*, 1981]. The phenomenon appears in the Northern and the Southern Hemispheres; however, the central period and amplitude of the two-day wave are slightly smaller in the Northern Hemisphere.

[3] Observations by single station measurements [e.g., *Harris*, 1994; *Palo et al.*, 1997; *Herman et al.*, 1999; *Fritts et al.*, 1999] and various satellite instruments [e.g., *Burks and Leovy*, 1986; *Wu et al.*, 1993, 1996; *Shepherd et al.*, 1999; *Lieberman*, 1999; *Azeem et al.*, 2001] reveal the two-day wave to be particularly strong in the mesosphere despite the presence of strong thermal damping (less than 0.2 days$^{-1}$) and mechanical damping (mainly gravity wave drag) at these altitudes [e.g., *Garcia*, 1989]. At low summer latitudes, the maximum meridional and zonal wind amplitudes are ~60 m/s and ~20 m/s, respectively. At middle summer latitude, the temperature wave amplitude can be greater than 5 K.

[4] Because of these large amplitudes, the two-day wave disturbance may also be present in chemical species like ozone and water vapor. Recently, *Azeem et al.* [2001] identified the wave signature in ozone and suggested it to be photochemically driven by the corresponding temperature perturbations through changes in reaction rates. However, global observations of the two-day wave disturbance in mesospheric water vapor do not exist. The lone previous observation of the two-day wave in water vapor was in the upper stratosphere by *Limpasuvan and Leovy* [1995]. In general, mesospheric water vapor has garnered much interest. Because it has strong vertical gradient in the upper mesosphere as a result of diminishing photochemical lifetime with altitude, water vapor serves as a great indicator for


0148-0227/03/2002JD002903$09.00

atmospheric transport [e.g., *Nedoluha et al.*, 1996; *Pumphrey and Harwood*, 1997]. Moreover, its presence is intimately linked to noctilucent clouds that appear over the extremely cold polar summer mesopause [e.g., *Garcia*, 1989, and references therein]. These clouds have been linked to increasing greenhouse gases and global change [e.g., *Olivero and Thomas*, 2001].

[5] In this paper, we present observations of the two-day wave disturbance in mesospheric water vapor and temperature. Such a study may shed additional light on the structure and mechanism of the two-day wave. To our knowledge, this study is the first to elucidate global two-day wave signature in water vapor at the mesospheric level. In our results, the water vapor two-day wave signature dominates the total field (particularly where the meridional gradient of water is strong) and is consistent with baroclinic instability of the easterly jet. Additionally, mixing of water vapor field by the two-day wave is suggested in the low summer latitudes through wave breaking processes.

## 2. Data and Analysis

[6] We use the newly available data of the Microwave Limb Sounder (MLS) [*Barath et al.*, 1993], an instrument on the Upper Atmosphere Research Satellite (UARS) [*Reber et al.*, 1993]. Launched in late 1991, the UARS is a sun-synchronous, polar orbiting satellite that completes ~14 orbits in a day. The water vapor mixing ratio is retrieved from the 180-GHz $H_2O$ line and extends approximately from 15 km to 90 km. As discussed by *Livesey et al.* [2003], the version (v5) data represents significant improvement and advancement in retrieval algorithm and processing software over previous MLS data versions. Subsequently, the v5 data has improved data quality and vertical resolution, particularly in the mesosphere. The temperature data is retrieved from $O_2$ 63-GHz emission with a separate algorithm (accounting for the geomagnetic Zeeman effect) and covers altitudes of 20–90 km [*Wu et al.*, 2003]. This retrieval uses a single temperature profile (an annual mean) as the first guess and linearization point.

[7] For analysis, we begin with the unbinned along-track vertical profiles (Level 3AT) of MLS mesospheric temperature and water vapor ($H_2O$) data. The vertical resolution of the $H_2O$ profiles is ~3 km in the stratosphere and ~5 km in the mesosphere. The vertical resolution for temperature is ~8 km in the stratosphere and ~14 km in the mesosphere. We then compute the spectra from the temperature and water vapor data at each level using the asynoptic mapping method of *Salby* [1982a, 1982b] to resolve signals with periods greater than 1 day. Application of this method to an earlier version of MLS data is discussed by *Elson and Froidevaux* [1993], *Canziani et al.* [1994], *Limpasuvan and Leovy* [1995], and *Lieberman* [1999].

[8] While the MLS data set is available from September 1991 to 1999, measurements after December 1994 are generally sparse, with no consecutive observations greater than 8 days [cf. *Livesey et al.*, 2003, Appendix]. As the asynoptic method is grounded on Fourier transform technique, a relatively long time series is necessary for acceptable spectral resolution and many cycles of the two-day wave. A time series of less than 8 days approximately contains only 112 measurements (i.e., 8 days at ~14 orbits a day) at a given latitude. After tapering 10% of the series at each end, the number of measurements is effectively reduced to ~90. To maintain relatively high spectral resolution, we avoid data after 1994. Furthermore, the UARS performs a yaw-around maneuver every 30–40 days (a "yaw period") to keep some instruments from pointing at the sun. The data spatial coverage is thus not truly global on a given day but rather extends from 80° latitude in one hemisphere to about 30° latitude of the other.

[9] As the two-day temperature wave (of zonal wave number 3) is previously observed mainly in the Southern Hemisphere during Austral summers, two relatively long data series are analyzed: (1) 15 January to 14 February 1992 and (2) 5 January to 8 February 1993. These data segments represent two yaw periods. The corresponding latitudinal coverage is between 80°S and 30°N. In practice, spatial coverage is limited to 28° and 68°. Data poleward of 68° is avoided because profiles taken during northward (or ascending) and southward (or descending) satellite paths become less distinct, causing numerical problems in the asynoptic mapping [*Lait and Stanford*, 1988].

[10] In the literature, the two-day wave is sometimes defined to include a wave number 4 disturbance with period of ~1.8 days [*Wu et al.*, 1996; *Lieberman*, 1999; *Limpasuvan et al.*, 2000a, 2000b]. During the Boreal summers (June–August) after the solstice, the wave number 4 generally dominates its wave number 3 counterpart and appears to be purely an instability mode. In the present paper, focus is placed strictly on the wave number 3 two-day wave, which is the dominant spectral signature for the chosen data segments (see below).

## 3. Results

### 3.1. Spectral Signature and Wave Structure

[11] Figure 1 shows the wave number-frequency spectra for water vapor and temperature in the mesosphere during the analyzed segments. The spectra are averaged between 70°S and 18°S and between 0.10 and 0.0046 hPa (65–86 km). Clearly, the dominant signature in both species is a westward-propagating, zonal wave number 3 disturbance with central period of ~2.1 days (about 0.48 cycles per day, cpd). The signal is consistent during each observed segment in the summer mesosphere. In this paper, we will refer to "two-day wave" as being associated with the spectral peak between 0.35 and 0.60 cpd (as noted in Figure 1).

[12] Figure 2 (top two rows) shows the amplitude distribution of the two-day wave in water vapor and temperature. Illustrated as filled contours, the wave amplitude is computed as the square root of the wave number 3, westward power spectra integrated over 1.67–2.86 days (0.35–0.60 cpd) at each level. The amplitude is plotted where the coherence squared with respect to the reference point is significant at the 95% level or greater (for approximately 5 degrees of freedom). This reference point is at the position where the amplitude is largest in the summer mesosphere (i.e., around 80 km and 40°S).

[13] Consistent with the spectral information, the temperature amplitude structure is mainly confined in the summer hemisphere and is remarkably similar in both years. Strongest magnitude appears around the midlatitude region of the upper mesopause (~80 km). Throughout much of the

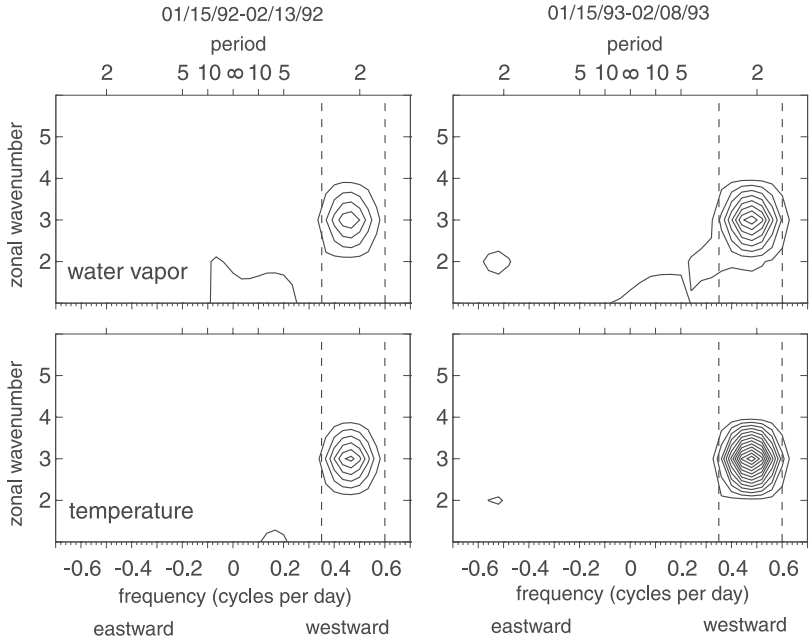


**Figure 1.** Spatially averaged power spectra of water and temperature between 70°S and 18°S and between 0.10 and 0.0046 hPa (approximately, 65–86 km). Water (temperature) contour interval is 0.0025 ppmv$^2$ (0.25 K$^2$) starting from 0.0025 ppmv$^2$ (0.25 K$^2$). The frequency range between 0.35 cycles per day (cpd) and 0.60 cpd (as marked by dashed lines) encompasses the two-day wave and is used for subsequent analyses.

mesosphere down to the stratopause, the wave amplitude structure tilts equatorward. A secondary maximum appears around 65 km. Near the stratopause (~50 km), the two-day wave amplitude is mostly in the subtropical region. These structures in the lower mesosphere and upper stratosphere concur with observations of previous versions of the MLS temperature data [*Limpasuvan and Leovy*, 1995; *Wu et al.*, 1996; *Limpasuvan et al.*, 2000a]. Finally, we note that the strength of the two-day wave amplitude is slightly stronger during 1993.

[14] The two-day wave in the water vapor data has a similar amplitude distribution as the temperature. A relatively strong peak appears near the mesopause level, but is more equatorward with respect to the temperature peak near the same level. As with the temperature data, the amplitude peak is stronger during the 1993 observations. Wave signature in the lower mesosphere is also evident in water vapor and is slightly equatorward of the peak aloft. During the 1992 observations, the peak in water vapor amplitude near the 50 km level has comparable strength to the amplitude near the mesopause. Such strong two-day wave signature in water vapor near the stratopause was noted by *Limpasuvan and Leovy* [1995] for the same year.

[15] Also shown in Figure 2 are distributions of MLS gravity wave variances observed around the same time interval as the two-day wave. These variances measure gravity wave activities at short horizontal (~100 km) but long vertical (>10 km) scales, providing additional information on atmospheric variability and instability. Details of MLS gravity wave retrievals are discussed by *Wu and Waters* [1996a, 1996b]. During the periods of interest, the gravity wave variance increases along the easterly jet core, similar to the variation of the two-day wave amplitudes, showing the poleward tilt as height increases. Again consistent with the two-day wave, the gravity wave variance is generally larger in 1993 than in 1992. Further discussions on gravity wave are provided in section 4.

[16] The meridional cross-section description is essentially only a time average representation of the wave structure during each of the chosen data segments. In general, the wave evolution appears to be episodic (i.e., pulse-like) and subsequently its structure can be variable (compare Figures 4–5). Examining the structure over the entire yaw periods results in a weak (or ''smeared'') representation of the wave structure. In addition, given the wave's episodic nature, a clean meridional cross-section representation of the wave phase structure over the 20–30 day interval is difficult to obtain [cf. *Burks and Leovy*, 1986; *Limpasuvan and Leovy*, 1995]. Therefore, to elucidate the wave phase structure we can simply examine the perturbation field associated with the two-day wave in height-longitude sections and longitude-latitude sections during the time of strongest wave activity. Here, the perturbation is obtained by integrating the wave number 3 spectra over the westward frequency range illustrated in Figure 1.

[17] Figure 3 demonstrates the wave phase for 26 January 1992. Nearly identical phase structure is observed in the 1993 observation (see also Figure 8). The phase of the two-day wave generally tilts westward with height above 60 km; this westward tilt is more obvious in the temperature results. Such westward vertical tilt is indicative of upward energy propagation for planetary-scale waves as determined by their dispersion relation if the zonal wave number is taken to be positive [*Andrews et al.*, 1987]. In the meridional direction, the wave phase tilts westward in the northward direction throughout the summer hemisphere. Such a hor-

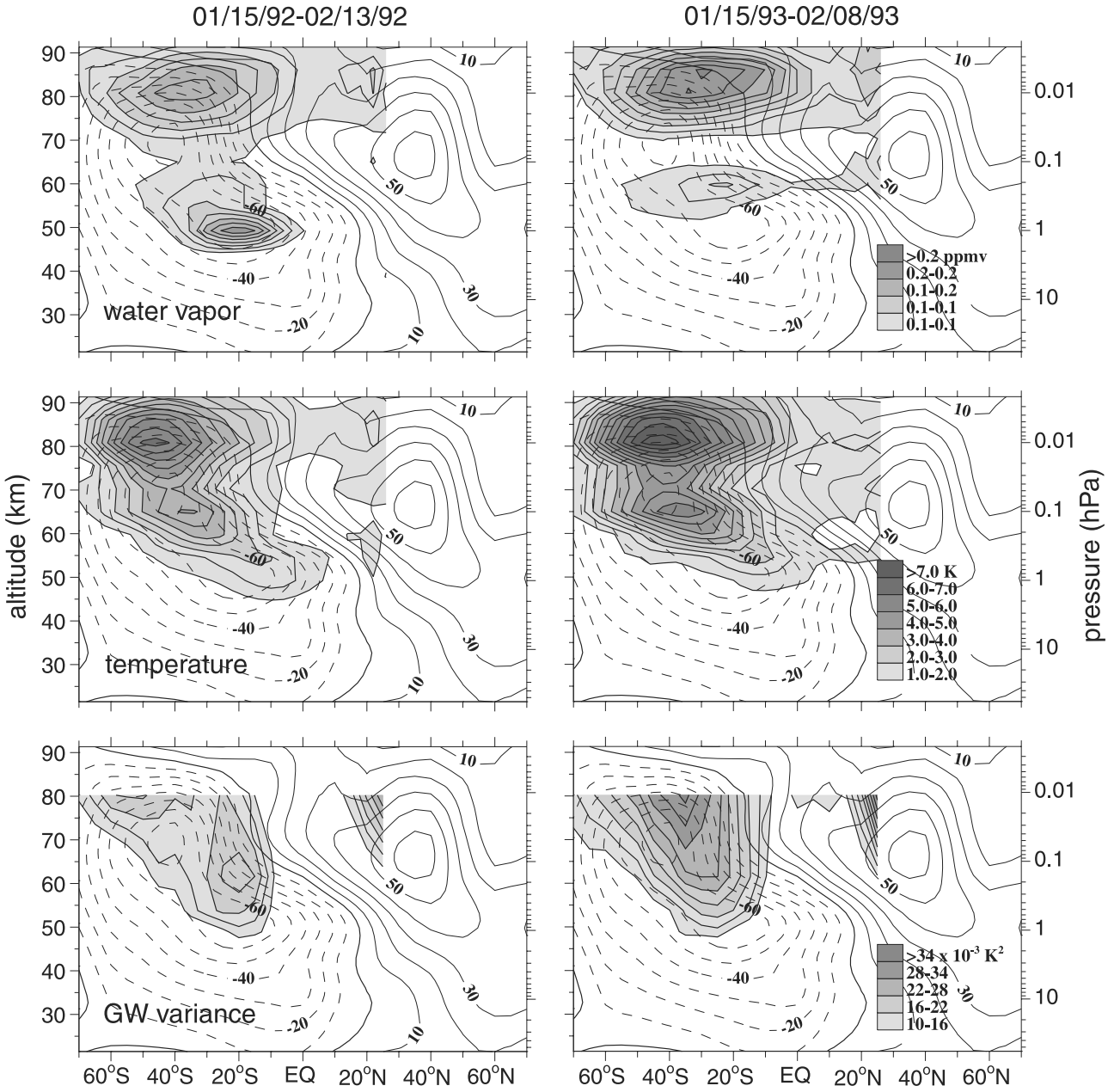


**Figure 2.** Meridional cross-sections of the two-day wave amplitudes. The wave amplitudes are given as filled contours. The CIRA mean zonal wind is superimposed as unfilled contours. The top (middle, bottom) row is for water vapor (temperature, gravity wave variance). The left (right) column is for analyzed period during 1992 (1993).

izontal phase structure is consistent with equatorward propagation of the two-day wave energy based on the Eliassen-Palm (EP) flux consideration [*Andrews et al.*, 1987].

### 3.2. Time Evolution

[18] The episodic nature of the two-day wave in the mesosphere is shown in Figure 4. The two-day wave amplitude is plotted as a function of latitude and time at 0.01 hPa (about 80 km). The wave amplitude can reach as high as 0.35 ppmv for water vapor and 11 K for the temperature. Remarkably, the amplitude variation of the water vapor wave nearly parallels that of the temperature wave. In particular, during January–February 1992, near-concurrent wave peaks appear around 20 January, 27 January, and 6 February. Consistent with the amplitude structure (compare Figure 2), the water vapor amplitude is slightly equatorward of the temperature amplitude.

[19] To highlight the relationship between water vapor and temperature waves, we compute the temporal correlation of their wave amplitudes at each height and latitude (see Figure 5). Correlation greater than 0.5 appears near the midlatitude, mesopause region and near subtropical, middle mesosphere (near 60 km). Around 80 km and 40°S, the correlation value exceeds 0.90 for both years. High correlation value means that the strength of temperature and water vapor wave perturbation tends to peak at the same time as

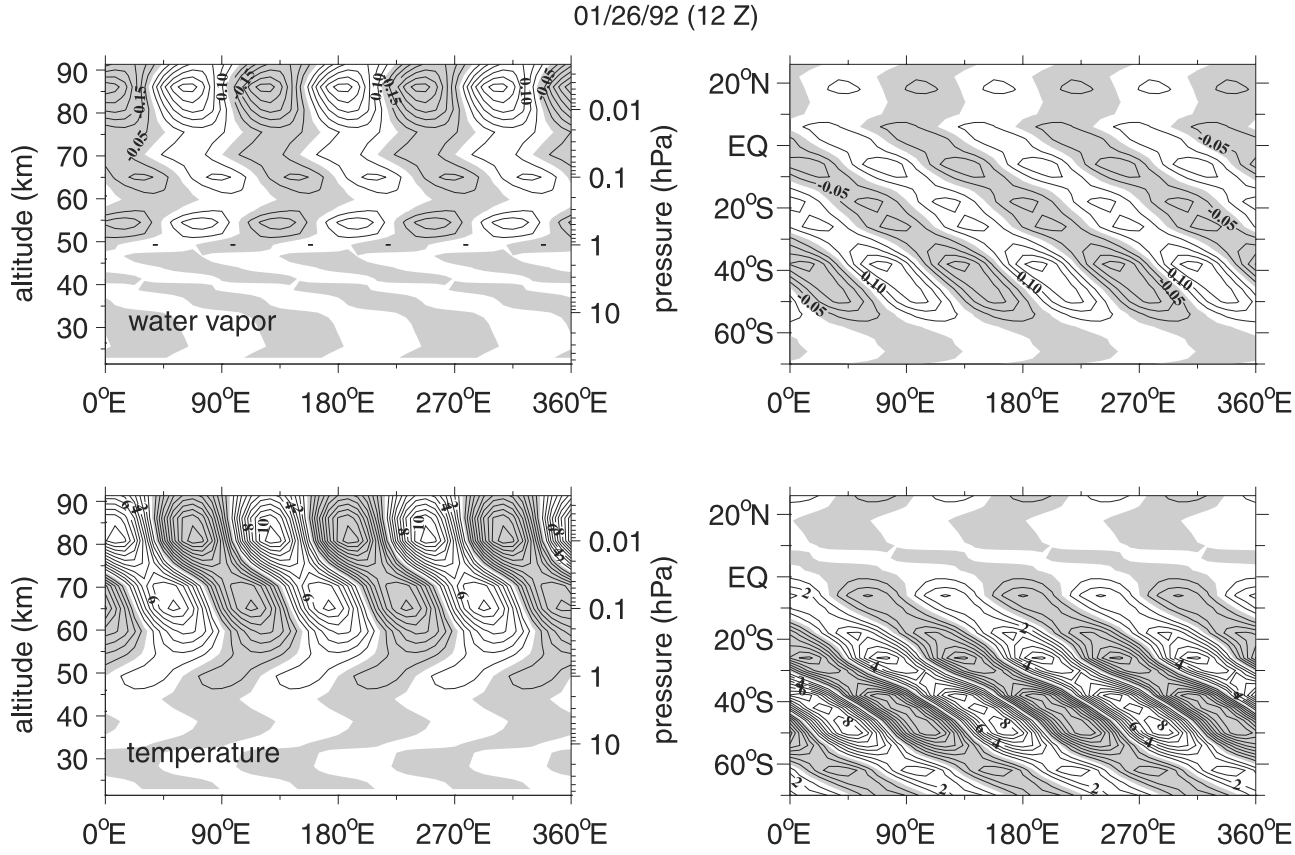


**Figure 3.** Two-day wave perturbations for water (top row) and temperature (bottom row) during 26 January 1992. The left column shows the longitude-height section at 38°S. The right column shows the longitude-latitude section at 0.01 hPa (∼80 km). These wave structures are also observed in 1993. Negative perturbations are shaded.

noted in Figure 4. However, such temporal correlation value does not reveal the relative phase of the wave amplitude.

[20] The relative phase difference between the temperature and water vapor wave is given in the bottom two rows of Figure 5. The phase difference is related to the difference in the longitudinal positions of the wave perturbation extrema. For zonal wave number 3 disturbance (such as the two-day wave), a 60° displacement in longitudes between the wave extrema corresponds to an out-of-phase (or 180° phase difference) relationship. Near the mesopause (0.01 hPa), the observed phase difference tends to be 180° during the entire observed time of each year. This out-of-phase relationship is apparent for all latitudes between 30°–46°S. In fact, this phase difference is apparent in Figure 3 as the shaded regions (negative perturbations) tend to overlap the unshaded regions (positive perturbations). At lower altitude (e.g., 60 km), where the temporal correlation values are generally smaller and $H_2O$ has longer photochemical timescale, the phase differences are more variable and, on average, are smaller than 180° (see bottom row of Figure 5). The tendency for this smaller phase shift is unclear.

## 4. Discussion

### 4.1. Structure and Instability

[21] Overall, the wave amplitude resides near the top side of the summer easterly jet core where the zonal wind can be in excess of 70 m/s on a day-to-day basis. To get a sense of the corresponding wind structure, we superimpose onto Figure 2 the CIRA climatological zonal wind [*Fleming et al.*, 1990] averaged for January and February (unfilled contours). Clearly, the wave amplitudes tend to collocate with regions of strong vertical and meridional wind shear that are typically just equatorward or above the easterly jet core. Strongest wave peak near the mesopause coincides with the levels where the easterly jet closes off (about 80–90 km).

[22] As mentioned in the Introduction, the described strong wind shears have led previous authors to link the two-day wave to barotropic/baroclinic instability (e.g., more recently by *Lieberman* [1999] and *Fritts et al.* [1999]). These studies show that the zonal mean wind structure exhibits regions of reversed potential vorticity gradient near the summer easterly jet core. Theoretically, *Plumb* [1983] and *Pfister* [1985] demonstrated that the fastest growing unstable mode with a westward propagating period of near two days is possible for a reasonably realistic easterly jet structure.

[23] However, the present MLS data coupled with the discussed limitations of the asynoptic mapping method largely exclude observations in the winter hemisphere. Subsequently, a global picture of the two-day wave is not presented in this study. Therefore the wave number 3 Rossby-gravity normal mode which exhibits an out-of-

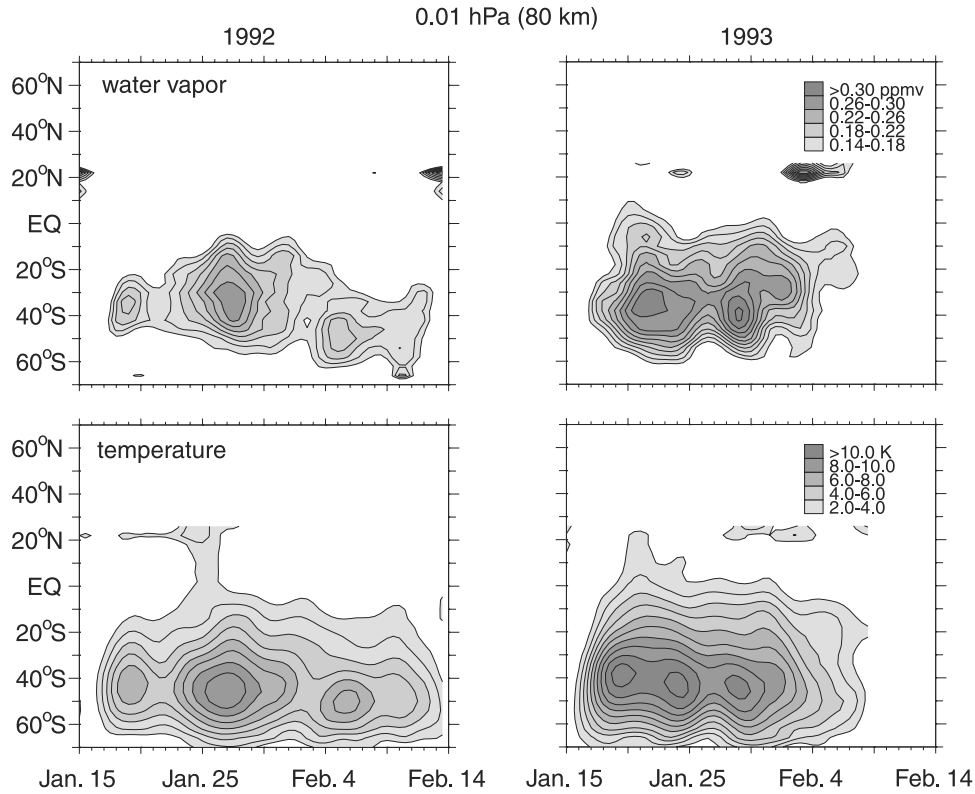


**Figure 4.** Two-day wave amplitude evolution at 0.01 hPa (about 80 km). Top (bottom) row is for water vapor (temperature). Left (right) column is for year 1992 (1993).

phase and weakened amplitude in the winter hemisphere around the solstice cannot be ruled out as an explanation of the observed two-day wave. Complete understanding of the two-day wave requires perhaps the perspectives of normal mode and instability theories [e.g., *Randel*, 1994; *Norton and Thuburn*, 1996].

[24] Throughout the mesosphere, gravity wave breaking provides strong eastward forcing to decelerate the easterly jets and likely accounts for the wind shears. Indeed, the westward acceleration by gravity wave forcing helps cap the summer easterly jets near the mesopause and drives the summer to winter pole circulation at those levels [*Leovy*, 1964; *Andrews et al.*, 1987]. The connection of gravity waves in the mesosphere with the two-day wave was demonstrated in the modeling work of *Norton and Thuburn* [1996, 1997]. In those studies, the simulated two-day wave amplitude structure, the region of westward forcing by gravity waves, and areas of reversed potential vorticity gradient collocate along the equatorward flank of the easterly jet with the upward tilt toward the summer pole. When the wind shear was weakened by introducing weaker gravity wave drag, the two-day wave was noticeably absent. Remarkably, the double peak wave structure of the temperature field observed here (see Figure 2) is very similar to the modeled results of Norton and Thuburn in both its latitude and altitude location.

[25] Gravity waves may play two roles in the two-day wave generation. First, strong wind shears emphasize the importance of gravity waves in accelerating the mean wind and setting up regions of instability for the two-day wave to proliferate. Second, by interacting with the background, gravity waves may directly provide a longtitudinally-varying drag in the upper mesosphere that could serve as the seed of instabiliy modes. The MLS variance maps show the gravity wave activities are highly varied in the Southern Hemisphere during December–Feburary because of convective and topographic sources in the lower atmosphere (not displayed).

[26] The phase structure of the two-day wave observed in this study suggests ties to instability. As illustrated in Figure 3, the phase tilt with height indicates upward energy propagation of the wave based on the dispersion relationship of planetary-scale waves. The upward energy propagation is consistent with the southern summer mesosphere observations of *Lieberman* [1999] and *Fritts et al.* [1999] who analyzed the High Resolution Doppler Image (HRDI) on UARS and single-station radar winds and temperature during 1992–1994. In these studies, the 2-day temperature perturbations are clearly out of phase with the meridional wind; therefore the heat flux ($\overline{v'T'}$) is negative. (Here, the overbar denotes zonal average, and the prime indicates departure from the zonal average.) The path of wave energy propagation can be related to the EP flux (***F***) whose vertical component is governed by heat flux [*Andrews et al.*, 1987]:

$$F_z \approx f_o \rho_o \overline{v'T'} \tag{1}$$

where $f_o$ is the Coriolis parameter and $\rho_o$ is the background density. Given the two-day temperature perturbation in the Southern Hemisphere during January–February, negative heat flux implies upward energy propagation. These studies also demonstrated the EP flux vectors to emanate from

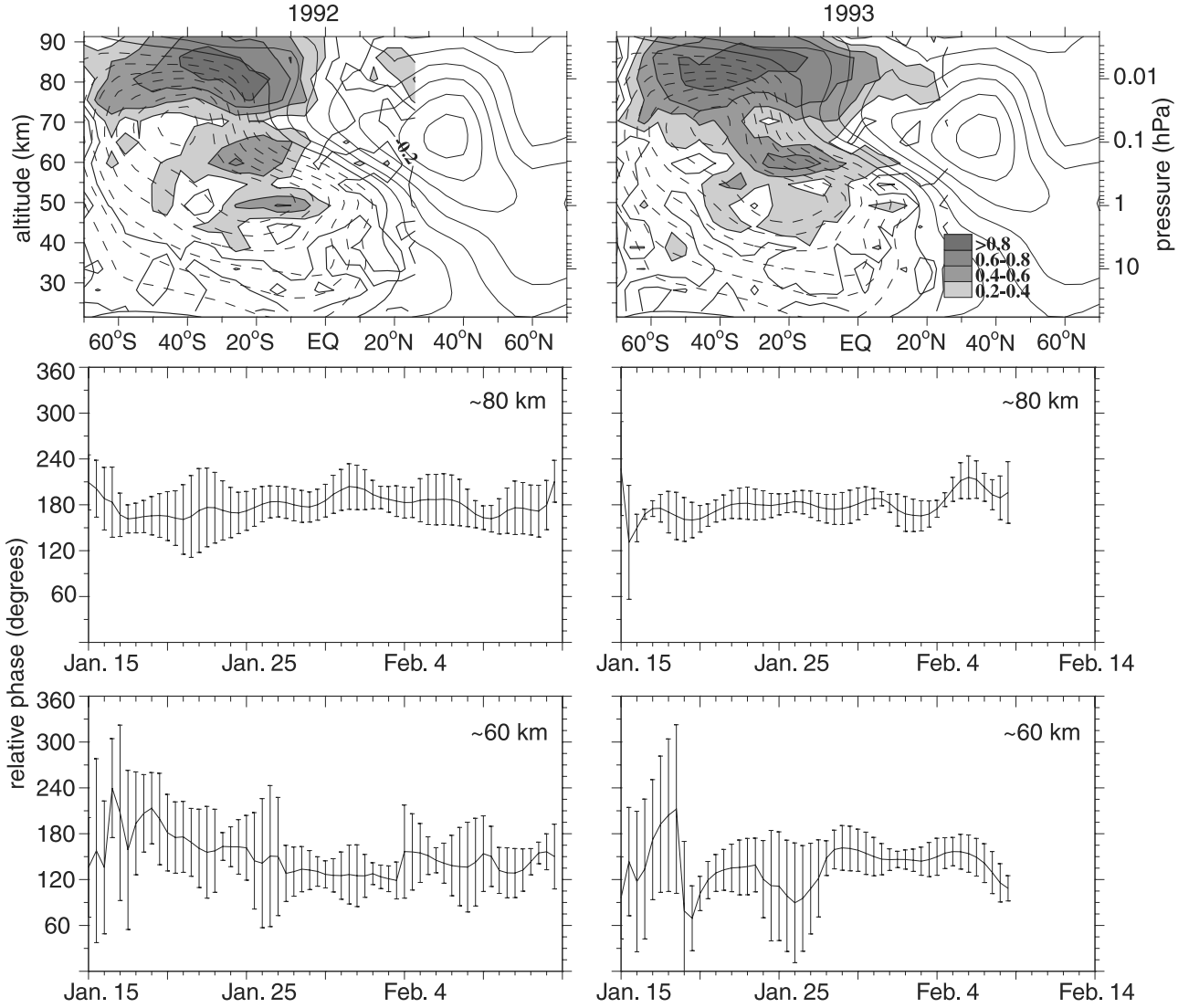


**Figure 5.** (Top row) Temporal correlation values of the two-day water vapor wave amplitude and two-day temperature wave amplitude. Regions where positive correlation values are greater or equal to 0.2 are shaded. (Middle row) Latitudinal averaged (30°S–46°S) phase difference between two-day water and temperature wave at 0.01 hPa (~80 km). The phase difference is the difference in longitudinal location of the wave perturbation peak. For zonal wave number 3, 180° phase difference corresponds to about 60° longitude displacement. The error bars denote phase differences that are one standard deviation away. (Bottom row) Same as the middle row except for 0.22 hPa (~60 km).

regions of negative potential vorticity gradient, suggesting a local wave source from the wave's critical line. Similar two-day wave energy radiation from an unstable region was modeled by *Limpasuvan et al.* [2000b].

### 4.2. Mean Tracer Gradient and Observed Amplitude

[27] Several daily cross-sections of the summer hemisphere $H_2O$ distribution are shown in Figure 6 around the time of strong two-day wave activity. Water vapor enters into the middle atmosphere typically through the cold tropical tropopause. In the stratosphere, water vapor is generated in situ by the oxidation of methane. Around the stratopause, nearly all methane is depleted and converted to water vapor. Above the stratopause, the water vapor concentration begins to diminish because of photodissociation due to absorption of solar radiation at wavelengths near Lyman $\alpha$ [e.g., *Nedoluha et al.*, 1996]. The lifetime of water molecules is on the order of several months near the stratopause; however, its lifetime at 80 km and above is only a few days [e.g., *Garcia*, 1989; *Pumphrey and Harwood*, 1997]. Generally, above 60 km, the distribution of water vapor is a result of the competition between transport (advective and diffusive) and photodisssociation. The vertical variation in lifetime accounts for strong vertical gradient in the water vapor field, particularly near the upper mesosphere.

[28] The observed latitudinal variation of water is however governed largely by vertical, advective transport. Below 50 km, the $H_2O$ distribution has an inverted Gaussian shape with minimum mixing ratio near the equator and

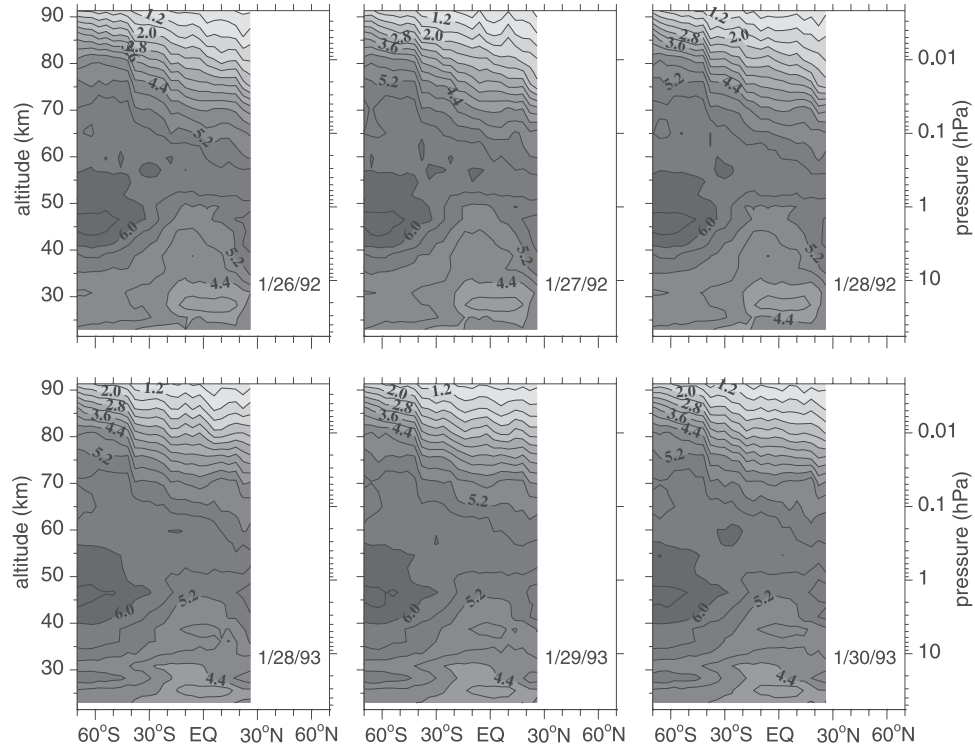


**Figure 6.** Selected meridional cross-sections of zonal mean water vapor during 1992 (top) and 1993 (bottom) when the two-day wave is relatively strong. Darker shading denotes wetter air.

relatively large concentration (greater than 7.0 ppmv) in the high summer latitudes. Such equatorial minimum in the distribution is consistent with a rising motion in the tropics that keeps the region relatively dry despite the presence of water vapor source due to methane oxidation throughout the stratosphere. Consequently, below 50 km, negative meridional gradient (decreasing concentration with latitude) is evident in the summer hemisphere and positive meridional gradient in the winter hemisphere.

[29] A relatively stronger negative meridional gradient in $H_2O$ exists in the midlatitude, upper summer mesosphere region ($\sim$80 km). This gradient is associated with an overturning mean meridional circulation driven primarily by gravity waves [e.g., *Garcia and Solomon*, 1985] in the mesosphere: with upwelling at the summer pole, meridional movement from the summer pole to winter pole, then downwelling at the winter pole. We note that the anomalously strong tracer gradient near 40°S between 70 and 90 km is probably an artifact of the MLS water data due to the a priori used for retrieving water. This aberration is obvious in all zonal mean cross-sections. In the winter hemisphere, the $H_2O$ distribution shows relatively weaker negative meridional gradient.

[30] During 1992, the meridional tracer gradient in the low summer latitudes (20°S–40°S) near the stratopause (40–50 km) is noticeably stronger than 1993. This enhanced meridional tracer gradient is associated with the presence of the 4.8–5.2 ppmv contour band at higher altitude (around 1 hPa) and is related to stronger upwelling in the equatorial upper stratosphere during 1992. This intense upwelling may be linked to the concurrent sudden warming episodes in the winter hemisphere [e.g., *Farman et al.*, 1994]. When intense warming occurs, strong wave forcing associated with dissipation of quasi-stationary waves (i.e., divergence of the EP flux) over the winter polar region drives an anomalously strong mean meriodional circulation, with rising over the equator and sinking over the winter pole [e.g., *Dunkerton et al.*, 1981; *McIntyre*, 1982]. In the $H_2O$ wave structure shown in Figure 2, the relatively strong amplitude in upper stratospheric region (1 hPa or about 50 km) during 1992 can perhaps be related to the difference in the described tracer gradient.

[31] The importance of background tracer gradient can be seen by considering the linearized continuity equation for a conservative tracer ($\chi$) in Cartesian coordinate ($x$, $y$, $z$) as given by *Andrews et al.* [1987]:

$$\left(\frac{\partial}{\partial t} + \bar{u}\frac{\partial}{\partial x}\right)\chi' + v'\bar{\chi}_y + w'\bar{\chi}_z = 0 \qquad (2)$$

Here, the subscript indicates partial derivative. Neglecting advection by vertical wind perturbation ($w'$), we can multiply the above equation by ($\chi'$), and take the zonally average to get:

$$\frac{\partial}{\partial t}\overline{\chi'^2} = -2\left(\overline{v'\chi'}\right)\left(\bar{\chi}_y\right) \qquad (3)$$

This equation states the dependence of the local time change of the tracer variance on the tracer meridional flux ($\overline{v'\chi'}$) and the background tracer meridional gradient ($\bar{\chi}_y$).

[32] For water vapor, equation (3) may be directly applicable in the lower mesosphere and upper stratosphere where

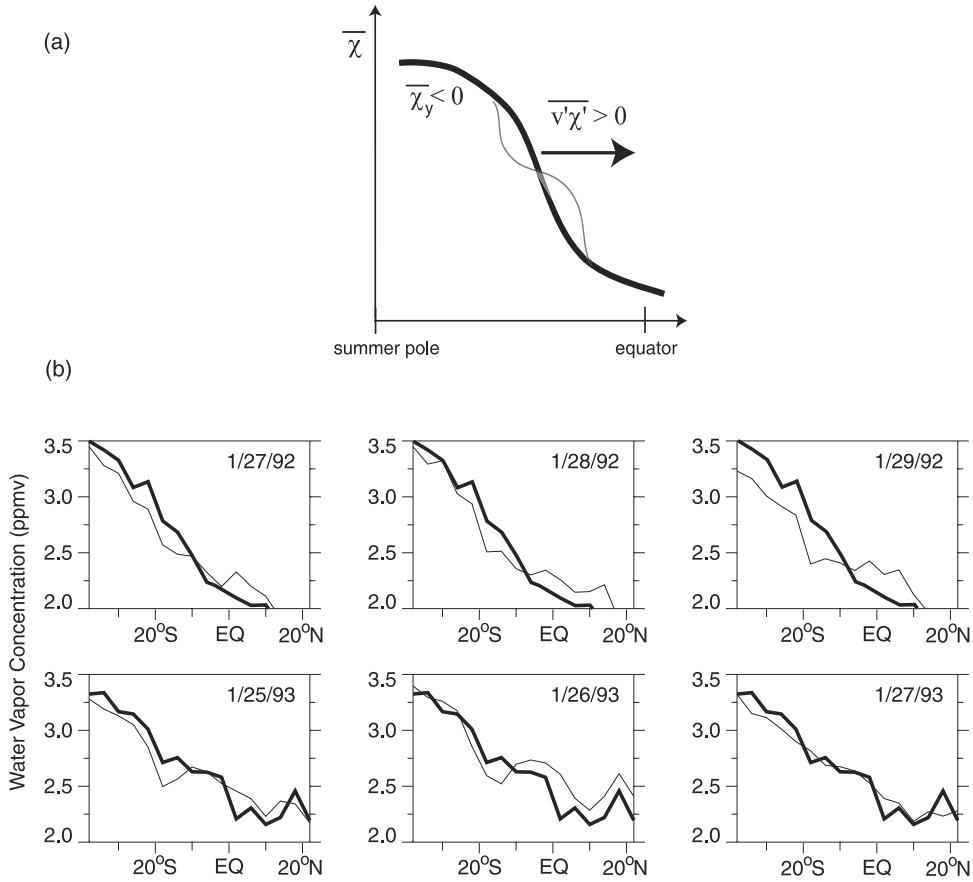


**Figure 7.** (a) A schematic of the latitudinal distribution of the zonal mean $H_2O$ tracer ($\chi$) during wave growth. The thick line is the background tracer distribution showing large midlatitude meridional gradient. The superimposed thin line is the perturbation as a result of the wave presence. Wave perturbations tend to alter the meridional gradient through equatorward flux of tracer. (b) Meridional profiles of water vapor at 80 km for 1992 and 1993. The thin lines are the profiles of the labeled dates; the thick lines in the top and bottom rows are for 23 January 1992 and 21 January 1993, respectively.

the chemical lifetime remains relatively long. Water vapor in that altitude range can be considered as a near-conservative tracer. However, the photochemical timescale of water becomes relatively small (about a few days) in the upper mesosphere, implying that water vapor is not truly conservative at these altitudes. As presented below, the above equation nonetheless qualitatively explains the $H_2O$ two-day oscillations near the mesopause.

[33] For a growing wave perturbation, the right hand side of equation (3) must be positive. Since the (background) meridional gradient of water vapor is always negative (see Figure 6), the associated wave flux must be down the mean tracer gradient resulting in equatorward or positive tracer flux in the summer hemisphere. This is shown schematically in Figure 7a for water vapor which has a minimum mixing ratio near the equator (see also Figure 6). Note that, while the equatorward tracer flux smooths out the pre-existing tracer gradient, it can also sharpen the gradient near adjacent latitudes.

[34] Such positive tracer meridional flux is consistent with the observed out-of-phase relationship between water vapor and temperature near the mesopause (see middle row of Figure 5). Recall that *Lieberman* [1999] and *Fritts et al.* [1999] found the temperature and meridional wind perturbations to be out of phase. This then implies that the meridional wind and water vapor perturbations must be in phase and ($\overline{v'\chi'}$) must be positive or equatorward. As illustrated in Figure 7b, sample meriodional profiles of the zonal mean water vapor at 80 km (where the two-day wave is strongest) indeed suggest changes in the low summer latitude (20°S to equator) profiles that are consistent with equatorward tracer flux. These profiles are shown when the two-day wave amplitude is large (see also Figure 4).

[35] Equation (3) also suggests that to observe strong wave amplitude in the tracer, relatively strong background meridional gradient of the tracer must be present. During 1992, stronger $H_2O$ wave amplitude is observed near 50 km because of a more pronounced background tracer gradient, despite comparable two-day wave signature in the 1993 temperature field. In association with the strong meridional gradient in the upper mesosphere, we also see a well-defined structure of the two-day wave in the water vapor field concentration near the high summer latitudes. For the same reasoning, we may attribute the diminished amplitude in the water vapor wave signature around the region of 55–

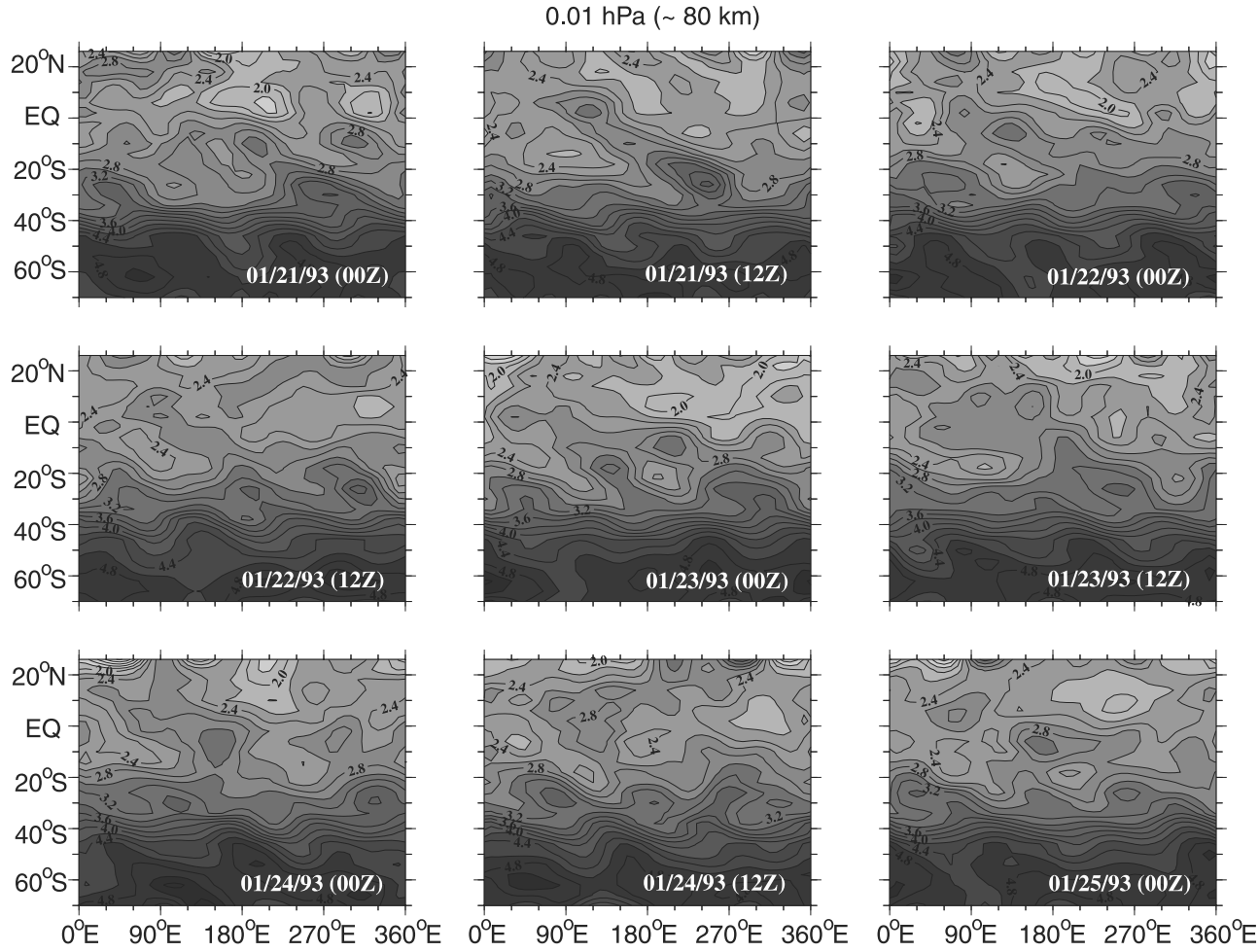


**Figure 8a.** Twice-daily maps of $H_2O$ during January 1993 at 0.01 hPa (~80 km). Darker shading denotes wetter air.

65 km to the weak gradient in the $H_2O$ field although the two-day temperature wave is quite strong.

### 4.3. Total Water Vapor Field and Possible Wave Breaking

[36] Figures 8a and 8b show the 1993 twice-daily maps of total water vapor at 0.01 hPa (~80 km) and 0.0046 hPa (~86 km), respectively, when the two-day wave is present (see Figure 4). Around 20°–60°S where the meridional tracer gradient is pronounced (see Figure 6), the two-day wave disturbance appears as zonal wave number 3 undulations in the isopleths that tilt westward to the north (consistent with Figure 3). Rearrangement of relatively moist (darker) and dry (lighter) air also occurs near 20°S as patches of moist (dry) air are observed equatorward (poleward) of 20°S. These latter features and the isopleth undulations are quite deep, appearing at both presented levels.

[37] On the basis of its large amplitudes, the two-day wave may break in the upper summer mesosphere in a manner similar to planetary waves in the winter hemisphere [*Plumb et al.*, 1987; *Limpasuvan and Leovy*, 1995; *Orsolini et al.*, 1997]. As noted by *Plumb et al.* [1987], given the large meridional displacement of the two-day wave coupled with the possibility of wave breaking, longer-lived constituents (lifetimes greater than 0.5 days) might exhibit a dramatic response in the mesosphere. Our observations of these water vapor maps suggest that wave breaking may indeed be occuring near the mesopause and may be associated with the two-day wave's amplitude decay observed in Figure 4.

[38] A dramatic wave breaking episode occurs around 21 January 1993, when the wave amplitude is very strong. A moist tongue extends from 270°E, 40°S to 90°E, EQ. At the same time, relatively dry air on the westward side of the moist tongue protrudes into the summer midlatitudes. After 21 January when breaking had occurred, we note several isolated dark and light "blobs" in the subtropics and diminished wave number 3 undulation near 40°S (see also Figure 4). After 23 January, the wave number 3 undulation again becomes pronounced and amplifies. This continued growth culminates into what appears to be another breaking feature around 90°E around 25 January (see Figure 8b). We note that these breaking episodes near the location of strong gradient is reminiscent of the tropical "surf zone" in the winter stratosphere [e.g., *Polvani et al.*, 1995].

## 5. Summary

[39] The two-day wave disturbance is identified throughout the mesosphere using the temperature and water vapor

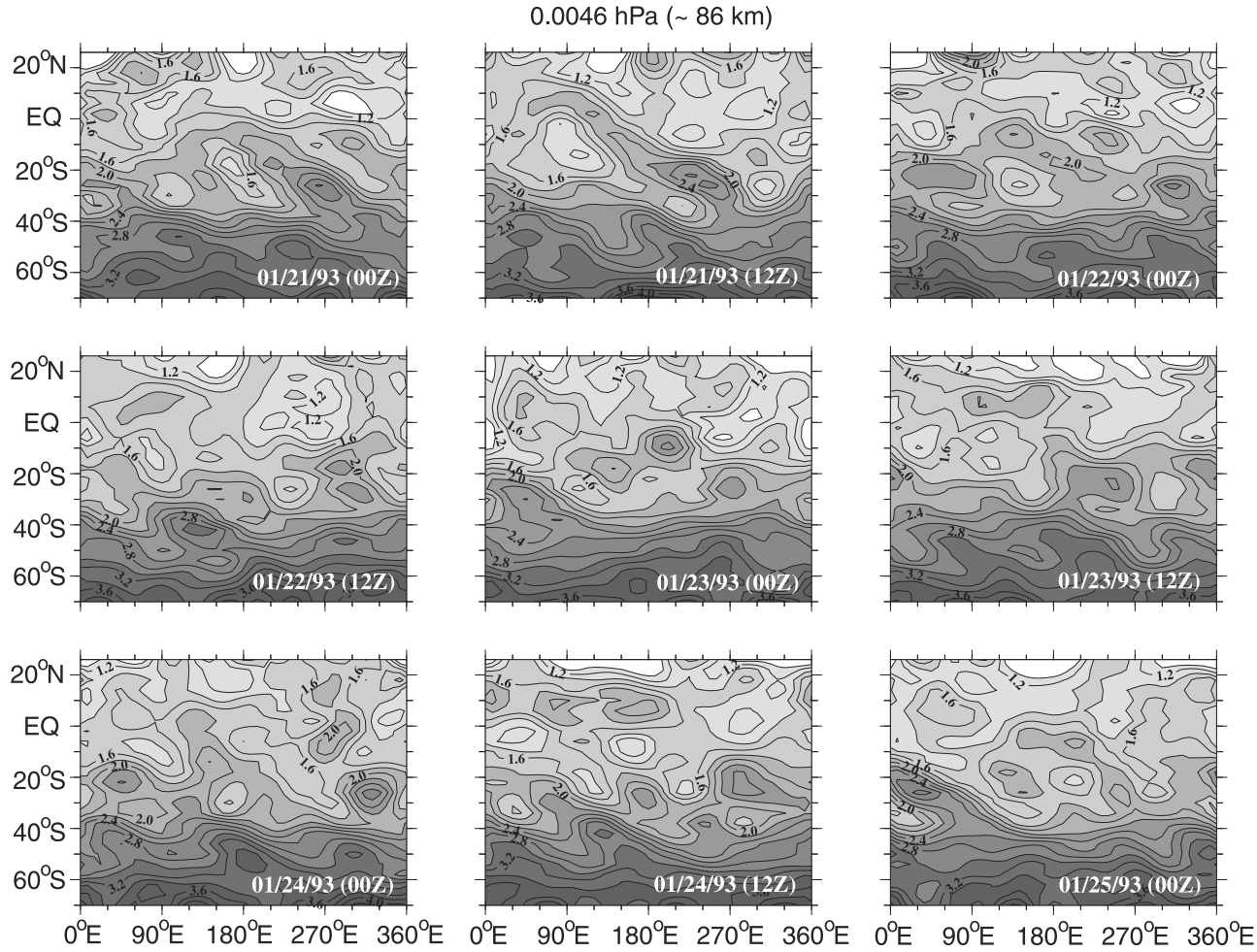


**Figure 8b.** Twice-daily maps of $H_2O$ during January 1993 at 0.0046 hPa (~86 km). Darker shading denotes wetter air.

measurements from the UARS MLS during two Austral Summers (January–February of 1992 and 1993). The spectral signature is in agreement with previous observations at lower altitudes, namely of zonal wave number 3 and a period of ~2 days. The disturbance is episodic during the observational periods of interest.

[40] The wave amplitudes are located near the core of the summer easterly jet with strongest wave amplitudes (about 11 K and 0.35 part per million by volume) near the mesopause where the easterly jet closes off. In these regions, gravity wave forcing can account for the strong vertical and meridional shear in the jet and may serve as a seed of instability.

[41] The water vapor and temperature perturbation strengths are highly correlated in time. This coherence extends throughout much of the mesosphere and from the middle to lower latitudes. However, the perturbation amplitudes tend to be nearly out of phase longitudinally. Such phase displacement is more robust in the upper mesosphere but less clearly defined in the lower mesosphere.

[42] The wave structure suggests instability as the cause for the wave appearance. Previous studies of the two-day wave during the same time period generally find an out-of-phase relationship between temperature perturbation and meridional wind perturbation, as expected for poleward heat flux or upward energy propagation. The observed wave phase tilts westward with height which is in agreement with upward propagating planetary waves.

[43] Despite relatively short photochemical lifetime in the upper mesosphere, the two-day wave presence in water vapor is consistently found in regions of strong meridional gradient. In 1992, when the $H_2O$ meridional gradient is larger in the upper stratosphere (apparently due to stronger equatorial upwelling during January–February) than 1993, a more pronounced two-day wave signature is detected in water vapor. Where the background tracer field is more or less homogeneous, the wave disturbance is not readily observable in water vapor even when a strong temperature wave ampltiude is evident.

[44] The two-day wave signature readily appears in the twice-daily maps of total water vapor as zonal wave number 3 isopleth undulations that tilt westward to the north. Near the mesopause, as the wave perturbations fully mature, features reminiscent of wave breaking are evident as overturning of extended tongues of moist and dry air. The wave breaking process subsequently leads to isolated patches of dry and moist air in the summer subtropics and diminished undulation of the water vapor isopleths.

[45] **Acknowledgments.** This study was supported initially in part by the South Carolina NASA Space Grant Consortium and was carried out when V.L. was a NASA Summer Faculty Fellowship at Jet Propulsion Laboratory (JPL). We are especially grateful to Joe W. Waters for hosting V.L. and Linda Rodgers for coordinating this Fellowship program. We are thankful for the assistance of Robert P. Thurstans, Jonathan H. Jiang, Yibo Jiang, and Paul Wagner at JPL. Finally, we are indebted to two anonymous reviewers, whose suggestions and comments significantly improved the initial draft of this manuscript.

## References

Andrews, D. G., J. R. Holton, and C. B. Leovy, *Middle Atmosphere Dynamics*, 489 pp., Academic, San Diego, Calif., 1987.

Azeem, S. M. I., S. E. Palo, D. L. Wu, and L. Froidevaux, Observations of the 2-day wave in the UARS MLS temperature and ozone measurements, *Geophys. Res. Lett.*, *28*, 3147–3150, 2001.

Barath, F. T., et al., The Upper Atmosphere Research Satellite Microwave Limb Sounder instrument, *J. Geophys. Res.*, *98*, 10,751–10,762, 1993.

Burks, D., and C. B. Leovy, Planetary waves near the mesospheric easterly jet, *Geophys. Res. Lett.*, *13*, 193–196, 1986.

Canziani, P. O., J. R. Holton, E. Fishbein, L. Froidevaux, and J. W. Waters, Equatorial Kelvin waves: A UARS MLS view, *J. Atmos. Sci.*, *51*, 3053–3076, 1994.

Dunkerton, T. J., C.-P. F. Hsu, and M. E. McIntyre, Some Eulerian and Lagrangian diagnostics for a model stratospheric warming, *J. Atmos. Sci.*, *38*, 819–843, 1981.

Elson, L. S., and L. Froidevaux, Use of Fourier transforms for asynoptic mapping: Application to the Upper Atmosphere Research Satellite Microwave Limb Sounder, *J. Geophys. Res.*, *98*, 23,039–23,049, 1993.

Farman, J. C., A. O'Neill, and R. Swinbank, The dynamics of the arctic polar vortex during the EASOE campaign, *Geophys. Res. Lett.*, *21*, 1195–1198, 1994.

Fleming, E. L., S. Chandra, J. J. Barnett, and M. Corney, Zonal mean temperature, pressure, zonal wind, and geopotential height as function of latitude, *Adv. Space Res.*, *10*(12), 11–59, 1990.

Fritts, D. C., J. R. Isler, R. S. Lieberman, M. D. Burrage, D. R. Marsh, T. Nakamura, T. Tsuda, R. A. Vincent, and I. M. Reid, Two-day wave structure and mean flow interactions observed by radar and High Resolution Doppler Imager, *J. Geophys. Res.*, *104*, 3953–3969, 1999.

Garcia, R. R., Dynamics, radiation, and photochemistry in the mesosphere: Implications for the formation of noctilucent clouds, *J. Geophys. Res.*, *94*, 14,605–14,615, 1989.

Garcia, R. R., and S. Solomon, The effects of breaking gravity waves on the dynamics and chemical composition of the mesosphere and lower thermosphere, *J. Geophys. Res.*, *90*, 3850–3868, 1985.

Harris, T. J., A long-term study of the quasi-two-day wave in the middle atmosphere, *J. Atmos. Terr. Phys.*, *56*, 569–579, 1994.

Herman, R. L., W. A. Robinson, and S. J. Franke, Observational evidence of quasi two-day wave interaction using MF radar, *Geophys. Res. Lett.*, *26*, 1141–1144, 1999.

Lait, L. R., and J. L. Stanford, Applications of asynoptic space-time Fourier transform methods to scanning satellite measurements, *J. Atmos. Sci.*, *45*, 3784–3799, 1988.

Leovy, C. B., Simple models of thermally driven mesosphere circulation, *J. Atmos. Sci.*, *21*, 327–341, 1964.

Lieberman, R. S., Eliassen-Palm fluxes of the 2-day wave, *J. Atmos. Sci.*, *56*, 2846–2861, 1999.

Limpasuvan, V., and C. B. Leovy, Observations of the two-day wave near the southern summer stratopause, *Geophys. Res. Lett.*, *22*, 2385–2388, 1995.

Limpasuvan, V., C. B. Leovy, and Y. J. Orsolini, Observed temperature two-day wave and its relatives near the stratopause, *J. Atmos. Sci.*, *57*, 1689–1701, 2000a.

Limpasuvan, V., C. B. Leovy, Y. J. Orsolini, and B. A. Boville, A numerical simulation of the two-day wave near the stratopause, *J. Atmos. Sci.*, *57*, 1702–1717, 2000b.

Livesey, N. J., W. G. Read, L. Froidevaux, J. W. Waters, M. L. Santee, H. C. Pumphrey, D. L. Wu, Z. Shippony, and R. F. Jarnot, The UARS Microwave Limb Sounder version 5 data set: Theory, characterization and validation, *J. Geophys. Res.*, *108*, doi:10.1029/2002JD002273, in press, 2003.

McIntyre, M. E., How well do we understand the dynamics of stratospheric warmings, *J. Meteorol. Soc. Jpn.*, *60*, 37–65, 1982.

McIntyre, M. E., On dynamics and transport near the polar mesopause in summer, *J. Geophys. Res.*, *94*, 14,617–14,628, 1989.

Nedoluha, G. E., R. M. Bevilacqua, R. M. Gomez, W. B. Waltman, B. C. Hicks, D. L. Thacker, and W. A. Matthews, Measurements of water vapor in the middle atmosphere and implications for mesospheric transport, *J. Geophys. Res.*, *101*, 21,183–21,193, 1996.

Norton, W. A., and J. Thuburn, The two-day wave in the middle atmosphere GCM, *Geophys. Res. Lett.*, *23*, 2113–2116, 1996.

Norton, W. A., and J. Thuburn, The mesosphere in the extended UGAMP GCM, in *Gravity Wave Processes and Their Parametrization in Global Climate Models*, vol. 50, edited by K. Hamilton, pp. 383–401, Springer-Verlag, New York, 1997.

Olivero, J. J., and G. E. Thomas, Evidence for changes in greenhouse gases in the mesosphere, *Adv. Space Res.*, *28*, 931–936, 2001.

Orsolini, Y. J., V. Limpasuvan, and C. B. Leovy, The tropical stratopause in the UKMO assimilated analyses: Evidence for a 2-day wave and inertial circulations, *Q. J. R. Meteorol. Soc.*, *123*, 1707–1724, 1997.

Palo, S. E., et al., An intercomparison between the GSWM, UARS, and ground based radar observations: A case-study in January 1993, *Ann. Geophys.*, *15*, 1123–1141, 1997.

Pfister, L., Baroclinic instability of easterly jets with applications to the summer mesosphere, *J. Atmos. Sci.*, *42*, 313–330, 1985.

Plumb, R. A., Baroclinic instability at the summer mesosphere: A mechanism for the quasi-two-day wave?, *J. Atmos. Sci.*, *40*, 262–270, 1983.

Plumb, R. A., R. A. Vincent, and R. L. Craig, The quasi-two-day wave event of January 1984 and its impact on the mean mesospheric circulation, *J. Atmos. Sci.*, *44*, 3030–3036, 1987.

Polvani, L. M., D. W. Waugh, and R. A. Plumb, On the subtropical edge of the stratospheric surf zone, *J. Atmos. Sci.*, *52*, 1288–1309, 1995.

Pumphrey, H. C., and R. S. Harwood, Water vapour and ozone in the mesosphere as measured by UARS MLS, *Geophys. Res. Lett.*, *24*, 1399–1402, 1997.

Randel, W. J., Observations of the 2-day wave in NMC stratospheric analyses, *J. Atmos. Sci.*, *51*, 306–313, 1994.

Reber, C. A., C. E. Trevathan, R. J. McNeal, and M. R. Lyther, The Upper Atmosphere Research Satellite (UARS) mission, *J. Geophys. Res.*, *98*, 10,643–10,647, 1993.

Salby, M. L., Rossby normal modes in nonuniform background conditions. part II: Equinox and solstice conditions, *J. Atmos. Sci.*, *38*, 1827–1840, 1981.

Salby, M. L., Sampling theory for asynoptic satellite observations, part I: Space-time spectra, resolution, and aliasing, *J. Atmos. Sci.*, *39*, 2577–2600, 1982a.

Salby, M. L., Sampling theory for asynoptic satellite observations, part II: Fast Fourier synoptic mapping, *J. Atmos. Sci.*, *39*, 2601–2614, 1982b.

Shepherd, M. G., W. E. Ward, B. Prawirosoehardjo, R. G. Roble, S. P. Zhang, and D. Y. Wang, Planetary scale and tidal perturbations in mesospheric temperature observed by WINDII, *Earth Planets Space*, *15*, 593–610, 1999.

Wu, D. L., and J. W. Waters, Gravity-wave-scale temperature fluctuations seen by the UARS MLS, *Geophys. Res. Lett.*, *23*, 3289–3292, 1996a.

Wu, D. L., and J. W. Waters, Satellite observations of atmospheric variances: A possible indication of gravity waves, *Geophys. Res. Lett.*, *23*, 3631–3634, 1996b.

Wu, D. L., O. B. Hays, W. R. Skinner, A. R. Marshall, M. D. Burrage, R. S. Lieberman, and D. A. Ortland, Observations of the quasi 2-day wave from the High Resolution Doppler Image on UARS, *Geophys. Res. Lett.*, *24*, 2853–2856, 1993.

Wu, D. L., E. F. Fishbein, W. G. Read, and J. W. Waters, Excitation and evolution of the quasi-2-day wave observed in UARS/MLS temperature measurements, *J. Atmos. Sci.*, *53*, 728–738, 1996.

Wu, D. L., et al., Mesospheric temperature from UARS MLS: Retrieval and validation, *J. Atmos. Sol. Terr. Phys.*, in press, 2003.

V. Limpasuvan, Department of Chemistry and Physics, Coastal Carolina University, P. O. Box 261954, Conway, SC 29528, USA. (var@coastal.edu)

D. L. Wu, Jet Propulsion Laboratory, California Institute of Technology, 4800 Oak Grove Drive, Pasadena, CA 91109, USA. (dwu@mls.jpl.nasa.gov)